



Phenol Degradation over Mesoporous-Assembled SrTi_xZn_{1-x}O₃ Nanocrystal Photocatalysts: Effects of metal loadings

Supachai Tiyawaraku^{*a}, Sumaeth Chavadej^{*a,b}, Pramoch Rangsunvigit^{a,b}

^aThe Petroleum and Petrochemical College, Chulalongkorn University, Chulalongkorn Soi12, Phayathai Rd., Pathumwan, Bangkok 10330, Thailand

^bNational Center of Excellence for Petroleum, Petrochemicals and Advanced Materials, Chulalongkorn Soi12, Phayathai Rd., Pathumwan, Bangkok 10330, Thailand
sumaeth.c@chula.ac.th

Advanced oxidation processes (AOPs) are effective techniques used to efficiently degrade non-biodegradable organic contaminants present in wastewater. Photocatalysis is an AOP that is very promising in the use of solar energy to initiate degradation reactions. The most interesting photocatalyst is SrTiO₃ since it is chemically stable, non-toxic, and highly active in hydrogen production. In this work, mesoporous-assembled SrTi_xZn_{1-x}O₃ nanostructure photocatalysts were synthesized by a sol-gel method with the aid of a structure-directing surfactant. The Ag, Cu, and Pt loadings on SrTi_xZn_{1-x}O₃ were carried out by the photochemical deposition method. The synthesized photocatalysts without and with different metal loadings were tested for the degradation of phenol, which was used as a model contaminant in water. The effects of various synthesis parameters, such as the ratio of Ti:Zn, calcination temperature, and metal loading content, on photocatalytic phenol degradation performance were investigated. The mesoporous-assembled photocatalyst SrTi_xZn_{1-x}O₃ nanostructure photocatalyst with a Ti-to-Zn molar ratio of 0.97:0.03 calcined at 700 °C provided the highest phenol degradation rate constant (k) of 0.80 h⁻¹. Among the studied loaded metals, Pt provided the highest photocatalytic activity toward phenol degradation.

1. Introduction

Nowadays, Environmental problem is a globally concerned topic. Several wastewaters are derived from the industrial processes. Organic compounds, such as phenol, are main contaminants in several industries such as petroleum refining, dyestuff, steel, coal tar, synthetic resins and liquefaction. Besides, phenol and phenolic compounds are also found to be used in daily life, such as disinfectants and veterinary medicine (Luenloi *et al.*, 2011). However, phenol and phenolic compounds have been reported to harm both environment and human health. Several treatment methods have been developed to eliminate phenolic compounds in wastewater, such as physical methods (adsorption), chemical oxidation, and biological treatment. However, the conventional processes for treatment of these phenol-containing effluents are ineffective to purify a large quantity of wastewaters. Photocatalysis technology has been widely investigated as an alternative and efficient AOP for pollutant eradication, with an emphasis on the development of effective photocatalysts (Puangpetch *et al.*, 2008). Therefore, several efforts have been studied to develop heterogeneous photocatalysts that can be efficiently used for degradation of organic contaminant. One of the most promising

Please cite this article as: Tiyawaraku S., Chavadej S. and Rangsunvigit P., (2012), Phenol degradation over mesoporous-assembled SrTi_xZn_{1-x}O₃ nanocrystal photocatalysts: effects of metal loadings, Chemical Engineering Transactions, 29, 1291-1296

photocatalysts is strontium titanate (SrTiO_3) because of its superior physicochemical properties, such as excellent thermal stability, high photocorrosion resistibility, and good structure stability as the host for metal ion doping (Ohno *et al.*, 2005). Khunrattanaphon *et al.* (2011) investigated the synthesis of $\text{SrTi}_x\text{Zr}_{1-x}\text{O}_3$ ($x = 0-1$) photocatalysts for photocatalytic degradation of acid black (AB) diazo dye, as a model contaminant. It was found that the photocatalyst with a proper Ti-to-Zr molar ratio could provide comparatively high photocatalytic efficiency. In this work, mesoporous-assembled $\text{SrTi}_x\text{Zn}_{1-x}\text{O}_3$ nanocrystal photocatalysts were synthesized by a sol-gel process. Experimental investigation was performed on the photocatalytic degradation of phenol as a model contaminant in wastewater. The effects of various synthetic parameters, including Ti-to-Zn molar ratio, calcination conditions for the photocatalyst preparation, and Ag, Cu, and Pt loadings on the photocatalytic phenol degradation performance were investigated.

2. Methodology

2.1 Materials for Experiments

Strontium nitrate ($\text{Sr}(\text{NO}_3)_2$, Merck Co. Ltd.), tetraisopropylorthotitanate (TIPT, Merck Co. Ltd.), acetylacetone (ACA, S.D. Fine-Chem Ltd.), zinc nitrate ($\text{Zn}(\text{NO}_3)_2 \cdot 6\text{H}_2\text{O}$, Ajax Finechem Pty. Ltd.), laurylamine (LA, Merck Co. Ltd.), hydrochloric acid (HCl, 37% analytical grade, Labscan Asia Co. Ltd.), anhydrous ethanol (EtOH, 99.5% purity, Italmar Co. Ltd.) were used as starting materials for synthesis of the $\text{SrTi}_x\text{Zn}_{1-x}\text{O}_3$ photocatalysts. Copper nitrate ($\text{Cu}(\text{NO}_3)_2 \cdot 2.5\text{H}_2\text{O}$, Ajax Finechem Pty. Ltd.), silver nitrate (AgNO_3 , Carlo Erba), platinum (IV) chloride acid hexahydrate ($\text{H}_2\text{PtCl}_6 \cdot 6\text{H}_2\text{O}$, Nacalai tesque) were used as cocatalyst precursors.

2.2 Photocatalyst Synthesis

The mesoporous-assembled $\text{SrTi}_x\text{Zn}_{1-x}\text{O}_3$ photocatalysts were synthesized via the sol-gel process. The TIPT and ACA were firstly mixed together and gently shaken until homogeneous mixing at room temperature to obtain the TIPT/ACA solution with various molar ratios of Ti-to-Zn to obtain different x values in the $\text{SrTi}_x\text{Zn}_{1-x}\text{O}_3$. Desired amounts of $\text{Sr}(\text{NO}_3)_2$ and Zinc nitrate (ZN) were dissolved in distilled water. Then, a proper amount of EtOH was added into the solution with a ratio of EtOH: H_2O of 3:2. After that, the surfactant solution of LAHC was added to the solution and continuously stirring at room temperature to obtain clear solution. Which was by then was slowly added to the TIPT-ACA solution while stirring continuously, where to obtain the molar ratios of (TIPT/ZN)-to-LAHC and (TIPT/ZN)-to-ACA of 4:1 and 1:1. The mixture was kept continuously stirring at 40 °C for 2 h to obtain transparent yellow sol. Then, the sol-containing solution was placed into an oven at 80 °C for a week in order to obtain complete gel formation. Accordingly, the gel was dried at 80 °C for 2 d. The dried gel was finally calcined at various temperatures (600–800 °C) for 4 h. Metal-loaded mesoporous-assembled $\text{SrTi}_x\text{Zn}_{1-x}\text{O}_3$ photocatalysts were prepared by a photochemical deposition (PCD) method. The $\text{SrTi}_x\text{Zn}_{1-x}\text{O}_3$ photocatalyst was dispersed in the 50 vol.% aqueous methanol solution and ultrasonicated for 15 min. Then, a desired amount of AgNO_3 , $\text{Cu}(\text{NO}_3)_2$, or PtCl_6 was added to the solution. The mixture was magnetically stirred and irradiated by a set of 11 W low-pressure Hg lamps (total light intensity of 44 W) for 3 h. After the irradiation, the metal-deposited photocatalyst powders were recovered by filtration, repeatedly washed with distilled water, and dried at 80 °C.

2.3 Photocatalyst Characterizations

The thermal decomposition behavior of the zero gels with the suitable thermal treatment conditions was investigated by using a thermogravimetric-differential thermal analyzer (TG-DTA). The N_2 adsorption-desorption isotherms were obtained by using a nitrogen adsorption-desorption apparatus. The Brunauer-Emmett-Teller (BET) approach was utilized to determine specific surface area. The structure and crystallinity of photocatalysts were examined by X-ray diffraction (XRD). The UV-visible spectrophotometer was used to record absorbance spectra of the photocatalysts. The photocatalyst morphologies and the existence of the metal loadings were observed by a transmission electron microscope (TEM).

2.4 Photocatalytic Activity Testing

The photocatalytic activity was performed in an open system at room temperature. Each experiment was carried out by taking a specified amount of each prepared photocatalyst to suspend in the phenol solution by using a magnetic stirrer within a reactor made of Pyrex glass. Prior to the photocatalytic activity test, the continuously suspended mixture was left for 30 min in a dark environment to establish the adsorption equilibrium. The reaction was started by exposing the mixture with UV light irradiation by 11 W mercury lamps. The suspension was periodically withdrawn and then centrifuged to separate the photocatalyst powders from the solution. The filtered liquid samples were analyzed by UV-visible spectrophotometer to follow its degradation. The pseudo-first order reaction kinetics was used to obtain apparent reaction rate constant of phenol degradation reaction.

3. Results and Discussion

3.1 Photocatalyst Characterization Results

3.1.1. TG-DTA Results

The DTA curves exhibited four main exothermic regions. The first exothermic peak is attributed to the removal of physisorbed water and ethanol molecules. The second exothermic peak between 150 and 300 °C is attributed to the burnout of the LAHC surfactant molecules. The third exothermic region between 300 and 425 °C corresponds to the removal of chemisorbed water molecules. The fourth region between 425 and 650 °C corresponds to the crystallization process of the photocatalyst. The TG curves reveal that the calcination temperature of approximately 650 °C was sufficient for both the complete surfactant removal and the photocatalyst crystallization for both dried photocatalysts.

3.1.2. N₂ Adsorption-Desorption Results

The adsorption-desorption isotherms of all of the samples exhibited typical IUPAC type IV pattern with a hysteresis loop, which is the main characteristic of a mesoporous material (mesoporous size between 2 and 50 nm), according to the classification of IUPAC (Rouquerol et al., 1999). The pore size distributions of all the synthesized photocatalysts were narrow in the mesoporous region, implying a good quality of the samples. The surface area and total pore volume of the synthesized SrTi_xZn_{1-x}O₃ photocatalysts (calcined at 700 °C for 4 h.) tended to increase (shown in Table 1) when increasing Zn molar ratio to 0.03 (i.e. SrTi_{0.97}Zn_{0.03}O₃) and then they decreased with further increasing Zn molar ratio. The results of textural properties of the metal loading, it can increase in the specific surface area from 20.6 to be higher than 33 m²·g⁻¹ (shown in Table 2). Moreover, with various Pt loadings, the results show that the specific surface area tended to increase with increasing Pt loading to reach a maximum value at 0.5 wt.% and then gradually decreased with further increasing Pt loading to 1 wt.%. However, the mean mesopore diameter remained almost unchanged at all Pt loadings in the investigated range.

3.1.3. XRD Results

With increasing Zn molar fraction of the mesoporous-assembled SrTi_xZn_{1-x}O₃ photocatalysts calcined at 700 °C, the dominant peak gradually shifted to a lower diffraction angle, confirming the presence of Zn in the form of solid solution. On the other hand, it was observed that the crystallite size of SrTi_{0.97}Zn_{0.03}O₃ photocatalyst increased from 19 to 26 nm (Table 1) as the calcination temperature increased from 600 to 800 °C. The metal loading SrTi_{0.97}Zn_{0.03}O₃ photocatalyst in the investigated range of 0-1.0 wt.% did not significantly affect the crystallite size of the SrTi_{0.97}Zn_{0.03}O₃ photocatalyst shows in Table 2

3.1.4. UV-Visible Spectroscopy Results

UV-visible spectroscopy was used to examine the light absorption ability of all synthesized photocatalysts. The absorption bands of the synthesized mesoporous-assembled SrTi_xZn_{1-x}O₃ photocatalysts were mainly in the UV light range of 200-400 nm with the band gap range of 3.12-3.20 eV (Table 1), and the absorption onset wavelength shifted to a shorter value with increasing Zn content. For each loaded metal (Ag, Cu, and Pt) on the SrTi_{0.97}Zn_{0.03}O₃ photocatalyst could contribute to the increase in light-harvesting ability within the visible light region (wavelength > 400 nm). However, the visible light response of photocatalysts did not pose any significant effect on their photocatalytic activity in this work.

Table 1: Textural properties of $\text{SrTi}_x\text{Zn}_{1-x}\text{O}_3$ photocatalysts from N_2 adsorption-desorption, XRD, UV-visible spectroscopy analyses

Photocatalyst	Calcination temperature (°C)	BET surface area ($\text{m}^2\cdot\text{g}^{-1}$)	Mean pore diameter (nm)	Total pore volume ($\text{cm}^3\cdot\text{g}^{-1}$)	Crystallize size (nm)	Band gap energy (E_g , eV)
SrTiO_3		11.5	3.90	0.042	27.029	3.12
$\text{SrTi}_{0.97}\text{Zn}_{0.03}\text{O}_3$		20.6	3.80	0.056	21.874	3.14
$\text{SrTi}_{0.95}\text{Zn}_{0.05}\text{O}_3$	700	7.7	3.78	0.024	20.890	3.15
$\text{SrTi}_{0.93}\text{Zn}_{0.07}\text{O}_3$		6.1	3.77	0.020	18.530	3.18
$\text{SrTi}_{0.91}\text{Zn}_{0.09}\text{O}_3$		5.2	3.77	0.018	17.993	3.20
	600	9.0	9.59	0.020	19.004	3.26
$\text{SrTi}_{0.97}\text{Zn}_{0.03}\text{O}_3$	700	20.6	3.80	0.056	21.874	3.14
	800	11.6	3.80	0.036	26.248	3.14

Table 2: Textural properties of metal loaded $\text{SrTi}_{0.97}\text{Zn}_{0.03}\text{O}_3$ photocatalysts from N_2 adsorption-desorption, XRD, UV-visible spectroscopy analyses

Photocatalyst	Metal loading (wt.%)	BET surface area ($\text{m}^2\cdot\text{g}^{-1}$)	Mean pore diameter (nm)	Total pore volume ($\text{cm}^3\cdot\text{g}^{-1}$)	Crystallize size (nm)	Band gap energy (E_g , eV)
	0	20.6	3.80	0.056	21.874	3.14
	0.5% Ag	33.0	3.80	0.063	23.189	3.02
	0.5% Cu	30.0	3.81	0.058	21.097	3.02
$\text{SrTi}_{0.97}\text{Zn}_{0.03}\text{O}_3$	0.25% Pt	33.0	3.82	0.067	21.213	3.06
	0.5% Pt	35.1	3.79	0.057	22.873	3.10
	0.75% Pt	34.8	3.83	0.069	20.727	3.13
	1% Pt	34.4	3.81	0.072	22.324	3.13

3.1.5. TEM-EDX Results

The morphologies of the SrTiO_3 and $\text{SrTi}_{0.97}\text{Zn}_{0.03}\text{O}_3$ photocatalysts are the cubic shape. The average particle sizes of the SrTiO_3 and $\text{SrTi}_{0.97}\text{Zn}_{0.03}\text{O}_3$ photocatalysts are in the range of 20-31 and 20-24.6 nm, respectively. These results showed that the particle sizes of the crystalline photocatalysts are similar to the crystallite sizes calculated from the XRD patterns by the Scherrer equation, indicating a single crystalline characteristic.

3.2. Photocatalytic AB Degradation Results

UV-visible spectroscopy was used to investigate the effects of various reaction parameters on the phenol degradation performance of all the synthesized $\text{SrTi}_x\text{Zn}_{1-x}\text{O}_3$ photocatalysts. As colorimetrically determined with 4-aminoantipyrine (Franson, 1989), the UV-visible spectra of phenol solutions reveal the λ_{max} value at 500 nm. The absorbances at this λ_{max} value were then used to investigate the phenol degradation.

3.2.1. Effect of Ti-to-Zn molar fraction

In this research, the mesoporous-assembled $\text{SrTi}_x\text{Zn}_{1-x}\text{O}_3$ photocatalysts synthesized with various Ti-to-Zn molar ratios were used to study the phenol degradation performance. The results of photocatalytic phenol degradation are shown in Figure 1(a). It can be observed that the reaction rate constant increased with increasing Zn content and reached a maximum value at 3 mol % (i.e. $\text{SrTi}_{0.97}\text{Zn}_{0.03}\text{O}_3$). However, it significantly decreased with further increasing Zn content higher than 3 mol%. Hence, the synthesized mesoporous-assembled $\text{SrTi}_{0.97}\text{Zn}_{0.03}\text{O}_3$ photocatalyst provided the highest photocatalytic activity ($k = 0.808 \text{ h}^{-1}$). The photocatalytic activity results can be explained by the specific surface area results (Table 1) that the incorporation of Zn with its suitable content of 3 mol% enhanced the specific surface area of the $\text{SrTi}_{0.97}\text{Zn}_{0.03}\text{O}_3$ photocatalyst, implying its higher surface

active reaction sites and lower probability of charge carrier recombination. However, the observed results of the decreased reaction rate constant at Zn contents higher than 3 mol% can be explained by their lower specific surface areas, leading to lower surface active reaction sites, as well as their very small crystallite sizes (Table 1), leading to higher probability of charge carrier recombination at the surface. Therefore, the synthesized mesoporous-assembled $\text{SrTi}_{0.97}\text{Zn}_{0.03}\text{O}_3$ photocatalyst was selected for further experiments.

3.2.2. Effect of calcination temperature

The photocatalytic activity results of the $\text{SrTi}_{0.97}\text{Zn}_{0.03}\text{O}_3$ photocatalyst calcined at various temperatures between 600 and 800 °C are shown in Figure 1(b). It was found that the reaction rate constant increased with increasing calcination temperature and reached a maximum value at 700 °C. However, when the calcination temperature exceeded 700 °C, the reaction rate constant decreased. These can be explained that an increase in the calcination temperature in the range of 600-700 °C led to an increase in the specific surface area (Table 1) For the calcination temperature in the range of 700-800 °C, decreases in the specific surface area and band gap energy (Table 1) may possibly increase the probability of the charge carrier recombination at the bulk traps.

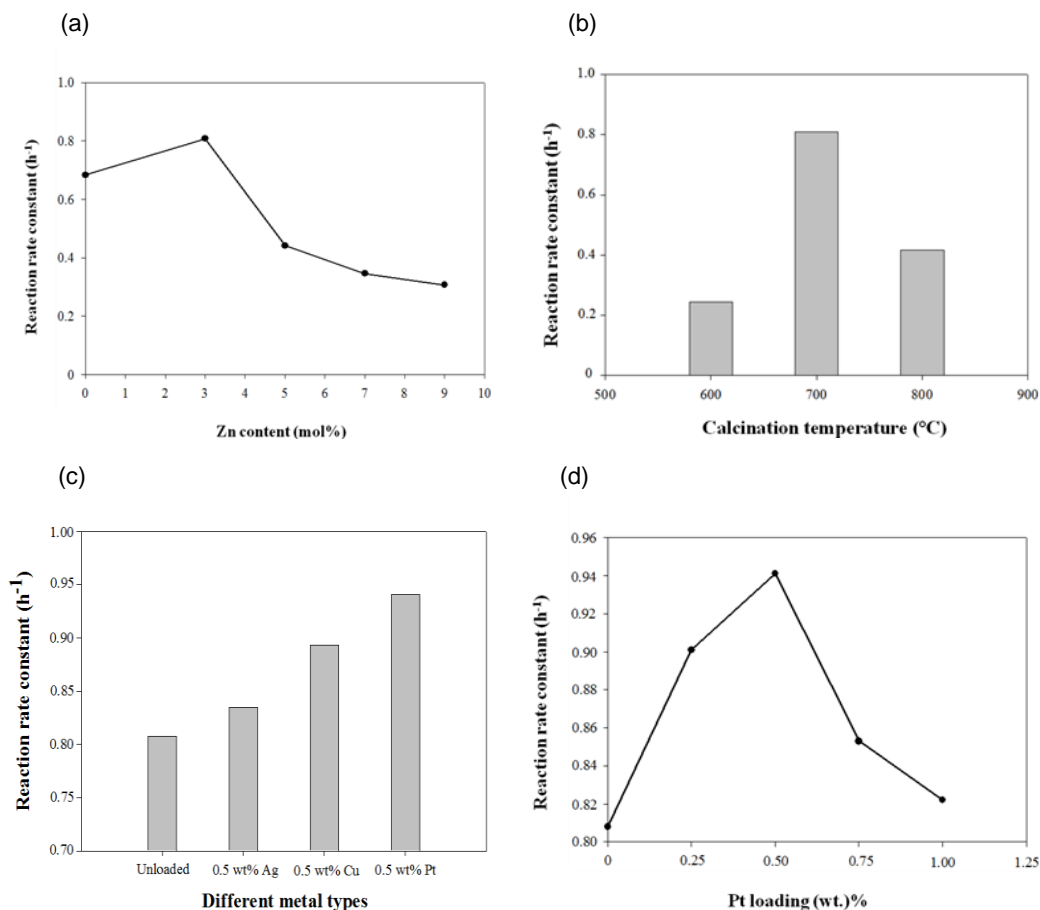


Figure 1: The reaction rate constant for phenol degradation of the synthesized $\text{SrTi}_x\text{Zn}_{1-x}\text{O}_3$ photocatalysts. (Photocatalyst 1 g; total reaction mixture volume, 200 ml; initial phenol concentration, 40 mg/l; and irradiation time, 4 h). (a) effect of Ti-to-Zn molar fraction, (b) effect of calcination temperature, (c) effect of different metal types, (d) effect of Pt Loading

3.2.3. Effect of different metal types

The mesoporous-assembled $\text{SrTi}_{0.97}\text{Zn}_{0.03}\text{O}_3$ photocatalysts loaded with different 0.5 wt.% metal types (i.e. Ag, Cu, and Pt) were comparatively used for the photocatalytic activity testing. The results of the

photocatalytic phenol degradation are shown in Figure 1(c). It can be clearly observed that all of the metals had a positive effect on the photocatalytic activity. The loaded metals can help accelerate the electron transfer and act as electron-capturing sites after band gap excitation to prevent the charge carrier recombination. However, the higher electronegativity of Pt nanoparticles possibly induces them to behave as more efficient active sites, which can hold electrons much better than the other metals, resulting in the highest photocatalytic activity of the Pt- loaded sample.

3.2.4. Effect of Pt Loading

The mesoporous-assembled $\text{SrTi}_{0.97}\text{Zn}_{0.03}\text{O}_3$ photocatalyst was used for further investigating the effect of Pt loading in the range of 0.25-1 wt.% on the photocatalytic phenol degradation. The results of the photocatalytic phenol degradation are shown in Figure 1(d). It was found that the reaction rate constant increased with increasing Pt loading to 0.5 wt.%, which provided the highest reaction rate constant of 0.941 h^{-1} ; however, it significantly decreased with further increasing Pt loading higher than 0.5 wt.%. It can be explained in that too much Pt loading resulted in a higher probability of the Pt nanoparticles to agglomerate and undesirably behave as recombination centers. In overall, the optimum Pt loading for the present investigated system was considered to be 0.5 wt.%.

4. Conclusions

In this research, the mesoporous-assembled $\text{SrTi}_x\text{Zn}_{1-x}\text{O}_3$ nanocrystal photocatalysts with various Ti-to-Zn molar ratios were synthesized by a sol-gel process and were used to investigate the photocatalytic phenol degradation. Among the investigated $\text{SrTi}_x\text{Zn}_{1-x}\text{O}_3$ photocatalysts, the mesoporous-assembled $\text{SrTi}_{0.97}\text{Zn}_{0.03}\text{O}_3$ was found to show the best photocatalytic phenol degradation activity. The effects of various synthetic parameters, including calcination conditions and metal loadings (Ag, Cu, and Pt), on the photocatalytic degradation performance of the synthesized mesoporous-assembled $\text{SrTi}_{0.97}\text{Zn}_{0.03}\text{O}_3$ photocatalyst were examined. The results showed that the presence of Pt on the $\text{SrTi}_{0.97}\text{Zn}_{0.03}\text{O}_3$ photocatalyst could greatly enhance the photocatalytic activity. The optimum conditions for synthesizing the effective $\text{SrTi}_{0.97}\text{Zn}_{0.03}\text{O}_3$ photocatalyst were a Pt loading of 0.5 wt.%, a calcination temperature of $700 \text{ }^\circ\text{C}$ providing the highest photocatalytic phenol degradation activity.

Acknowledgement

The authors would like to thank the Petroleum and Petrochemicals College, and the Center of Excellence on Petrochemical and Materials Technology, Chulalongkorn University, Thailand.

References

- Luenloi T., Chalermssinsuwan B., Sreethawong T., Hinchiranan N., 2011. Photodegradation of phenol catalyzed by TiO_2 coated on acrylic sheets: Kinetics and factorial design analysis, *Desalination*, 274, 192-199.
- Puangpetch T., Sreethawong T., Yoshikawa S., Chavadej, S., 2008. Synthesis and photocatalytic activity in methyl orange degradation of mesoporous-assembled SrTiO_3 nanocrystals prepared by sol-gel method with the aid of structure-directing surfactant, *Journal of Molecular Catalysis A: Chemical*, 287, 70–79.
- Ohno T., Tsubota T., Nakamura Y., Sayama K., 2005. Preparation of S, C cation-codoped SrTiO_3 and its photocatalytic activity under visible light, *Applied Catalysis A: General*, 288, 74–79.
- Khunrattanaphon P., Chavadej S., Sreethawong T., 2011. Synthesis and application of novel mesoporous-assembled $\text{SrTi}_x\text{Zr}_{1-x}\text{O}_3$ -based nanocrystal photocatalysts for azo dye degradation, *Chemical Engineering Journal*, 170, 292-307.
- Rouquerol F., Rouquerol J., Sing K., 1999. Adsorption by Powders and Porous Solid: Principle, Methodology and Applications, Academic Press, San Francisco, USA.
- Franson M.A.H., 1989. Standard method for the examination of water and waste water, American Public Health Association, 5-48-5-53.